

Available online at www.sciencedirect.comJOURNAL OF
COMPUTATIONAL AND
APPLIED MATHEMATICS

Journal of Computational and Applied Mathematics 204 (2007) 515–525

www.elsevier.com/locate/cam

A mixed hybrid formulation based on oscillated finite element polynomials for solving Helmholtz problems

Adrianna Gillman^{a,*}, Rabia Djellouli^a, Mohamed Amara^b^a*Department of Mathematics, California State University Northridge, Northridge, CA 91330, USA & MAGIC, Associate team of Magique-3D Inria Futurs, France*^b*Laboratoire de Mathématiques Appliquées, Université de Pau et des Pays de l'Adour & CNRS-FRE2570, BP 1155, 64013 PAU Cedex, France*

Received 14 October 2005; received in revised form 27 February 2006

Abstract

A mixed-hybrid-type formulation is proposed for solving Helmholtz problems. This method is based on (a) a local approximation of the solution by oscillated finite element polynomials and (b) the use of Lagrange multipliers to “weakly” enforce the continuity across element boundaries. The computational complexity of the proposed discretization method is determined mainly by the total number of Lagrange multiplier degrees of freedom introduced at the interior edges of the finite element mesh, and the sparsity pattern of the corresponding system matrix. Preliminary numerical results are reported to illustrate the potential of the proposed solution methodology for solving efficiently Helmholtz problems in the mid- and high-frequency regimes.

© 2006 Elsevier B.V. All rights reserved.

Keywords: Mixed and hybrid FEM; Discontinuous Galerkin method; Lagrange multipliers; Helmholtz problems; Wave number; Oscillated polynomials; Plane waves; Pollution effect

1. Introduction

The numerical solution of problems involving waves has been an area of active research for almost half of a century. This is due in part to the importance of applications that require a *practical* solution of wave phenomena problems such as sonar, radar, geophysical exploration, medical imaging, nondestructive testing, and more recently meteorology. Despite the tremendous progress that has been made in the recent years, this area is still regarded as one of the most challenging in scientific computation. The challenge of efficient computation at high wave numbers, in particular, has been designated as one of the problems still unsolved by current numerical techniques. Indeed, standard computational methods such as Galerkin finite element methods (FEM) are unable to cope with wave phenomena at short wavelengths because they require a prohibitive computational effort in order to resolve the waves and control numerical

* Corresponding author.

E-mail addresses: adrianna.m.gillman@csun.edu (A. Gillman), rabia.djellouli@csun.edu (R. Djellouli), mohamed.amara@univ-pau.fr (M. Amara).

dispersion errors. For example, solving an acoustic scattering problem using quadratic finite elements (Q_2 -element) for $ka = 10$, where k is the wave number and a characterizes the dimension of the considered submarine-like scatterer, requires solving a system with 10 millions complex unknowns [20] while sonar applications require solving these exterior Helmholtz problems for ka larger than 200. This simply rules out reliable solutions of the Helmholtz equation by the standard Galerkin FEM in the mid- and high-frequency regimes. Therefore, it is significant to develop discretization schemes that avoid or-at least-control effectively the dispersion and the so-called *pollution errors* [5] in order to be able to address practical problems.

In response to this challenge, numerous discretization techniques for alleviating the pollution effect in the standard Galerkin approach have been developed. These include the weak element method for the Helmholtz equation [19], the Galerkin/least-squares method [14], the quasi-stabilized FEM [3], the partition of unity method [4,17], the residual-free bubbles for the Helmholtz equation [12], the ultra-weak variational method [8,16], the least squares method [18], and recently a discontinuous Galerkin method designed by Farhat et al. and exposed in a series of papers [9–11].

We propose a mixed hybrid-type formulation [6] for solving Helmholtz problems in which the solution is approximated locally by *oscillated* finite element polynomials. In addition, the continuity across element boundaries of the solution is enforced weakly by Lagrange multipliers. The discontinuous nature of the approximation enables static condensation of primal variable prior to assembly. Consequently, the computational complexity of the proposed discretization method is determined mainly by the total number of Lagrange multiplier degree of freedom introduced at the edges of the finite element mesh, and the sparsity pattern of the corresponding system matrix. We must point out that the proposed method is very similar to the DGM formulation presented in [9]. The main difference between the two methods is in the approximation of the solution at the element level. Indeed, in the DGM approach the solution is approximated by *planar waves*.

The remainder of this paper is as follows. First, we specify notations and assumptions, and state the mathematical formulation of two-dimensional acoustic scattering problems in bounded domains. Next, we describe the proposed mixed hybrid method. Last, preliminary numerical results obtained in the case of two-dimensional wave guide and scattering problems are reported to illustrate the potential of the proposed method for solving mid- and high-frequency regimes Helmholtz problems.

2. Preliminary

We consider the time-harmonic scattering acoustic waves by an impenetrable *sound-hard* obstacle Ω . This problem can be formulated in a *bounded domain* Ω^c as the following boundary value problem (BVP):

$$(BVP) \quad \begin{cases} \text{Find } u \in H^1(\Omega^c) \text{ such that} \\ \Delta u + k^2 u = 0 & \text{in } \Omega^c, \\ \frac{\partial u}{\partial \mathbf{v}} = -\frac{\partial}{\partial \mathbf{v}} (e^{ik\mathbf{x} \cdot \mathbf{d}}) & \text{on } \Gamma, \\ \frac{\partial u}{\partial \mathbf{v}} - iku = 0 & \text{on } \Sigma, \end{cases} \quad (1)$$

where Ω^c is the computational domain containing Ω , Γ is the boundary of Ω assumed to be Lipschitzian, Σ is the exterior boundary of Ω^c assumed to be Lipschitzian, \mathbf{v} is the outward normal to the boundary of Ω^c , k is a positive number representing the wave number, and \mathbf{d} is unit vector representing the direction of the incident wave. Note that the couple (k, \mathbf{d}) characterizes the incident plane wave.

We must point out that the interior Neumann boundary condition on Γ and the exterior condition on Σ are used only for simplicity. The results presented herein apply to all types of admissible boundary conditions. Moreover, it is well-known that for practical problems, one should use *higher-order* local absorbing boundary conditions on Σ and not the condition in BVP (1) that we have chosen for simplicity only.

Finally, it is easy to show that this problem is well-posed in the sense of Hadamard, i.e., the solution u exists, is unique, and depends continuously with respect to scattering data.

3. The mixed-hybrid variational formulation

3.1. The continuous problem

Let \mathcal{T}_h be a regular triangulation of the computational domain Ω^c into subdomains K with boundary ∂K . The subdomain K is either a triangular-shaped or a quadrilateral-shaped element. h characterizes the step-size of the triangulation. Then, we adopt the following hybrid-type variational formulation for solving the BVP (1):

$$(VP) \begin{cases} \text{Find } (u, \lambda) \in X \times M \text{ such that} \\ a(u, v) + b(v, \lambda) = F(v) \quad \forall v \in X, \\ b(u, \mu) = 0 \quad \forall \mu \in M, \end{cases} \quad (2)$$

where the bilinear forms $a(\cdot, \cdot)$ and $b(\cdot, \cdot)$, and the right-hand side F are given by

$$a(u, v) = \sum_{K \in \mathcal{T}_h} \left(\int_K (\nabla u \cdot \nabla \bar{v} - k^2 u \bar{v}) dx - ik \int_{\partial K \cap \Sigma} u \bar{v} dt \right) \quad \forall u, v \in X \quad (3)$$

$$b(v, \mu) = \sum_{K \in \mathcal{T}_h} \int_{\partial K} \mu^K \bar{v} ds \quad \forall (v, \mu) \in X \times \mathcal{M} \quad (4)$$

$$F(v) = - \sum_{K \in \mathcal{T}_h} \int_{\partial K \cap \Sigma} \bar{v} \frac{\partial}{\partial \mathbf{v}} (e^{ik\mathbf{x} \cdot \mathbf{d}}) dt \quad \forall v \in X \quad (5)$$

X is the space of the *primal* variable. X is given by

$$X = \{v \in L^2(\Omega^b) \quad \forall K \in \mathcal{T}_h, v_K = v|_K \in H^1(K)\} \approx \prod_{K \in \mathcal{T}_h} H^1(K)$$

M is the space of the *dual* variable defined. M is given by

$$M = \left\{ \mu \in \prod_{K \in \mathcal{T}_h} H^{-1/2}(\partial K) \quad \forall \lambda \in T, \sum_{K \in \mathcal{T}_h} \langle \mu^K, \lambda^K \rangle_{-1/2 \times 1/2, \partial K} = 0 \right\},$$

where $\mu^K = \mu|_{\partial K}$ and the space T is given by

$$T = \left\{ \lambda \in \prod_{K \in \mathcal{T}_h} H^{1/2}(\partial K); \quad \forall K, K' \in \mathcal{T}_h, \lambda^K = -\lambda^{K'} \quad \text{on } \partial K \cap \partial K' \right\}$$

and \mathcal{M} is a subspace of M defined by $\mathcal{M} = M \cap \prod_{K \in \mathcal{T}_h} L^2(\partial K)$. Hence, we have

$$\left| \mathcal{M} = \left\{ \mu \in \prod_{K \in \mathcal{T}_h} L^2(\partial K); \quad \mu = 0 \text{ on } \partial\Omega^c \text{ and } \forall K, K' \in \mathcal{T}_h, \right. \right. \\ \left. \left. \mu^K + \mu^{K'} = 0 \text{ on } \partial K \cap \partial K' \right\} \right|.$$

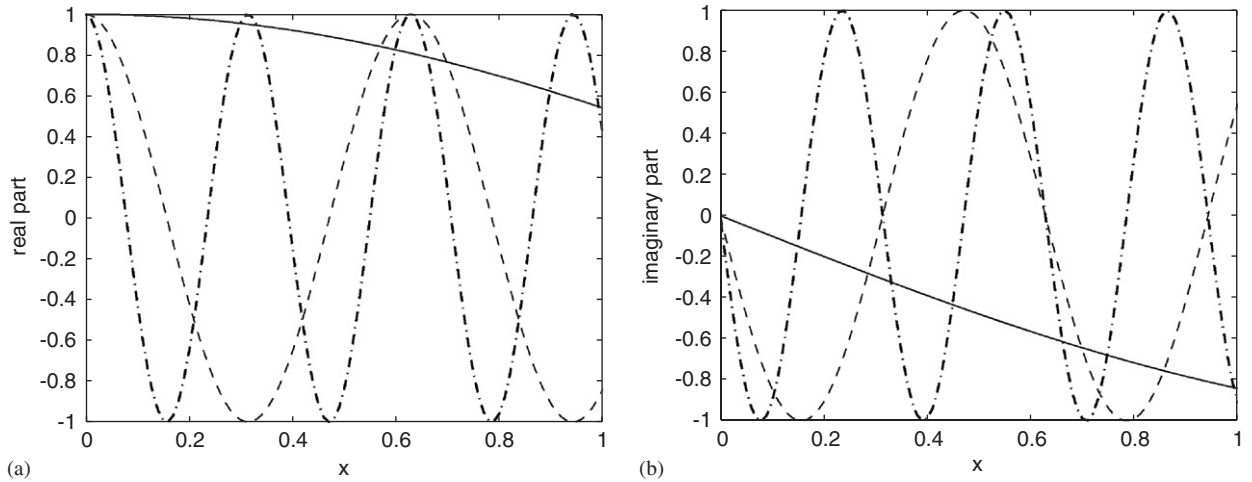


Fig. 1. Dependence of the one-dimensional shape function $\phi_1^K(x)$ with respect to the wave number: — $ka = 1$, --- $ka = 10$, and -·-·- $ka = 20$; (a) Real part of $\phi_1^K(x)$; (b) Imaginary part $\phi_1^K(x)$.

Note that the variational problem (VP) (2) has been already studied in [2] where the results on the existence and the uniqueness of the solution $(u, \lambda) \in X \times M$, as well as the stability results can be found.

3.2. The discrete problem

The method we propose is based on approximating the primal variable by oscillated finite element polynomials at the element level. For clarity purposes, we present the method in the context of triangular-shaped elements K with oscillated P_1 polynomials. Therefore, the discrete formulation corresponding to the VP (2) is given by

$$(DVP) \begin{cases} \text{Find } (u_h, \lambda_h) \in X_h \times M_h \text{ such that} \\ a(u_h, v_h) + b(v_h, \lambda_h) = F(v_h) \quad \forall v_h \in X_h, \\ b(u_h, \mu_h) = 0 \quad \forall \mu_h \in M_h. \end{cases} \quad (6)$$

The discrete space X_h for the primal variable is given by:

$$X_h = \left\{ v_h \in X; \quad \forall K \in \mathcal{T}_h, \quad v_h|_K = \sum_{j=1}^3 v_j^K \phi_j^K; \quad \text{where } v_j^K \in \mathbb{C} \right\},$$

where

$$\phi_l^K(x) = e^{-ikh_l A_l^K(x)}; \quad 1 \leq l \leq 3. \quad (7)$$

$A_l^K(x)$ is the *Lagrange polynomial* corresponding to the vertex s_l^K of the triangle K . The discrete space M_h for the dual variable is given by

$$M_h = \{\mu_h \in \mathcal{M}; \quad \forall K \in \mathcal{T}_h \text{ and } \forall T_j^K \subset \partial K : \mu_j^K = \mu_{|T_j^K} \in \mathbb{C}; \quad 1 \leq j \leq 3\},$$

where T_l^K ($l = 1, 2, 3$) represents the side opposite of vertex s_l^K of triangle K .

We must point out that the shape functions given by Eq. (7) have been chosen because they oscillate more and more as the wave number increases. This oscillatory aspect is clearly illustrated in Fig. 1 where we report the dependence of the shape function $\phi_1^K(x)$ with respect to the wave number in the one-dimensional case. Consequently, the oscillations of the solution of BVP (1) are already present in the local approximation of the solution. Therefore, it should be expected that this method has the potential to solve efficiently BVP(1) in mid- and high-frequency regime. On the other hand,

for practical applications, the oscillated aspect of the shape functions requires particular attention when computing the elementary integrals. There exists various schemes for integrating efficiently and accurately such integrals that we plan to use when implementing higher-order polynomials (see for example Ref. [7] among others). At this preliminary stage of the study, we have used Gauss–Legendre quadrature with up to 40 points (depending on the frequency) to perform the numerical experiments presented in the next section.

Furthermore, the corresponding algebraic linear system of DVP (6) can be statically condensed at the element level, so that only the degrees of freedom (dofs) corresponding to the Lagrange multiplier λ_h need to be assembled into a global linear system of equations where the unknowns are the λ_h dofs only. Hence, the computational complexity of the proposed method is determined mostly by the total number of Lagrange multiplier dofs introduced at the edges of the mesh elements, and the sparsity pattern of the resulting matrix. Note that the stencil width of the resulting condensed matrix is 5 in the case of triangular-shaped elements and 7 in the case of quadrilateral-shaped elements. Because of the size of the linear systems resulting in all the numerical experiments we have performed so far (about half million of unknowns for the largest one), we have solved these systems using an *LU* factorization procedure [15] with a compressed sparse row storage.

4. Numerical illustration

We present in this section, the results of two sets of numerical experiments to illustrate the potential of the method for solving Helmholtz problems in the mid- and high-frequency regime.

4.1. Performance assessment

We report here on the performance of the proposed method in the case of two-dimensional interior and exterior Helmholtz problems.

4.1.1. Wave guide problems

We have performed a numerical investigation to assess the potential of the method for solving two-dimensional wave guide problems in the mid- and high-frequency regime. More specifically, we consider here an $a \times a$ square-shaped domain, and solve the Helmholtz equation with boundary conditions such that the exact solution u^{ex} of the resulting problem is a plane wave propagating in a given direction $\mathbf{d} = (\cos \theta^*, \sin \theta^*)$, i.e.:

$$u^{\text{ex}} = e^{ik\mathbf{d} \cdot \mathbf{x}}. \quad (8)$$

Note that this problem is representative of interior Helmholtz problems. We vary the angle of propagation θ^* in the interval $[0, 2\pi)$ and compute the solution of the corresponding problem by solving the proposed mixed-hybrid variational formulation using a uniform *triangular*-shaped mesh. Then, for each angle θ^* , we assess the accuracy of the proposed method by evaluating the relative error using the following *modified* H^1 -norm.

$$\|u - u^{\text{ex}}\|_{\widehat{H}^1(\Omega)} = \left(\sum_K \|u - u^{\text{ex}}\|_{H^1(K)}^2 + \sum_{\partial K \in \mathcal{T}_h} \|u_{K'} - u_K\|_{L^2(\partial K \cap \partial K')}^2 \right)^{1/2}. \quad (9)$$

This norm takes into account the jump in the solution along the element edges. We have also computed the *total* relative error by evaluating the *mean* relative error over all angle of propagation θ^* in the interval $[0, 2\pi)$. The total relative error can be viewed, to some extent, as a relative error on a superposition of plane waves-type solution of an interior Helmholtz problem.

Preliminary numerical results are reported in Figs. 2–3(b). These results are obtained for various wave number ka and mesh resolution h/a . The following three observations are noteworthy:

- a. Fig. 2 illustrates (i) the dependence of the mean relative error with respect to the propagation angles, and (ii) the pollution effect of the proposed method. More specifically, we observe the following:
 - i. As expected from the expression of the exact solution (see Eq. (8)), the relative error is symmetric with respect to propagation angle π . For all three frequencies ka and step sizes h/a , the relative error in the interval $[0, \pi)$ is minimal at the propagation angle $\theta^* = 35^\circ$ (about 6%), and is maximal at $\theta^* = 95^\circ$ (less than 10%).

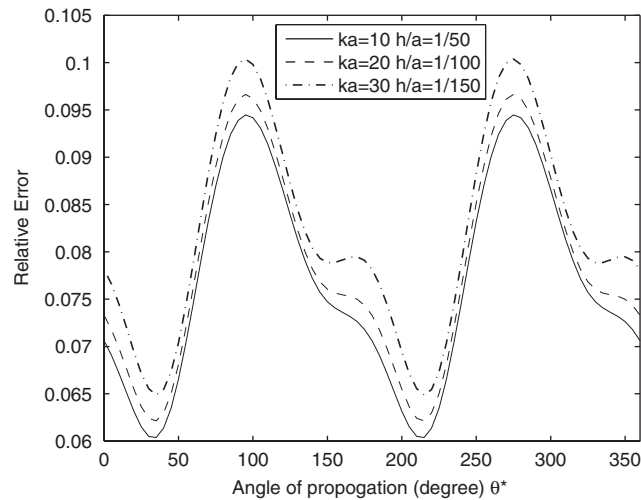
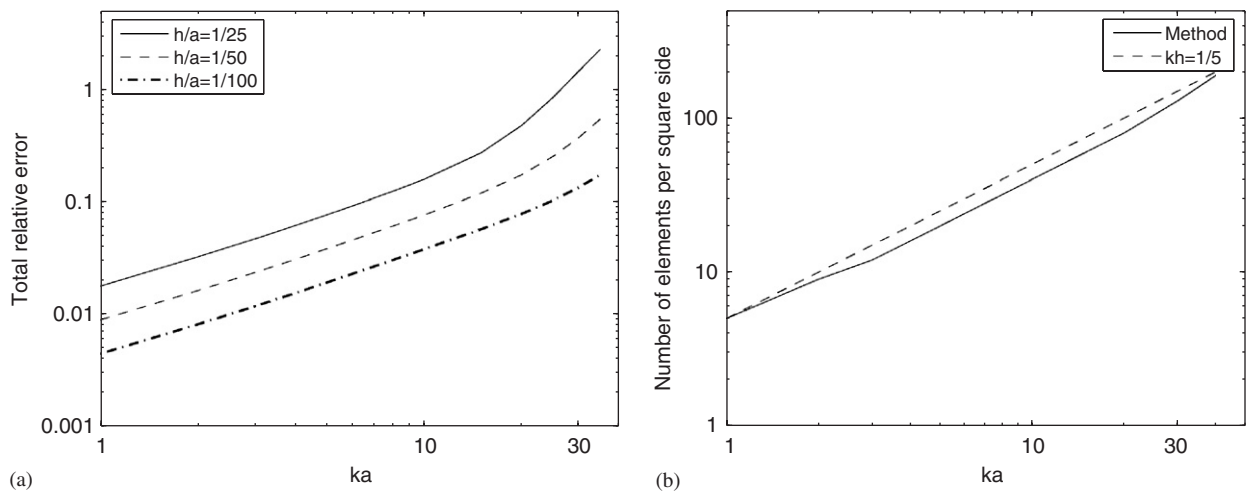
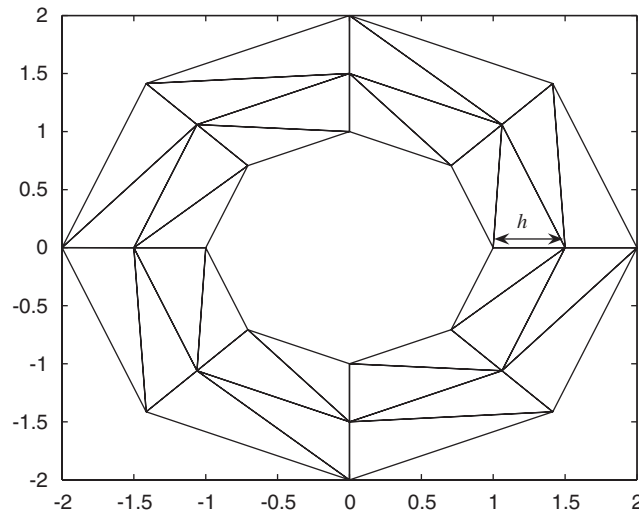
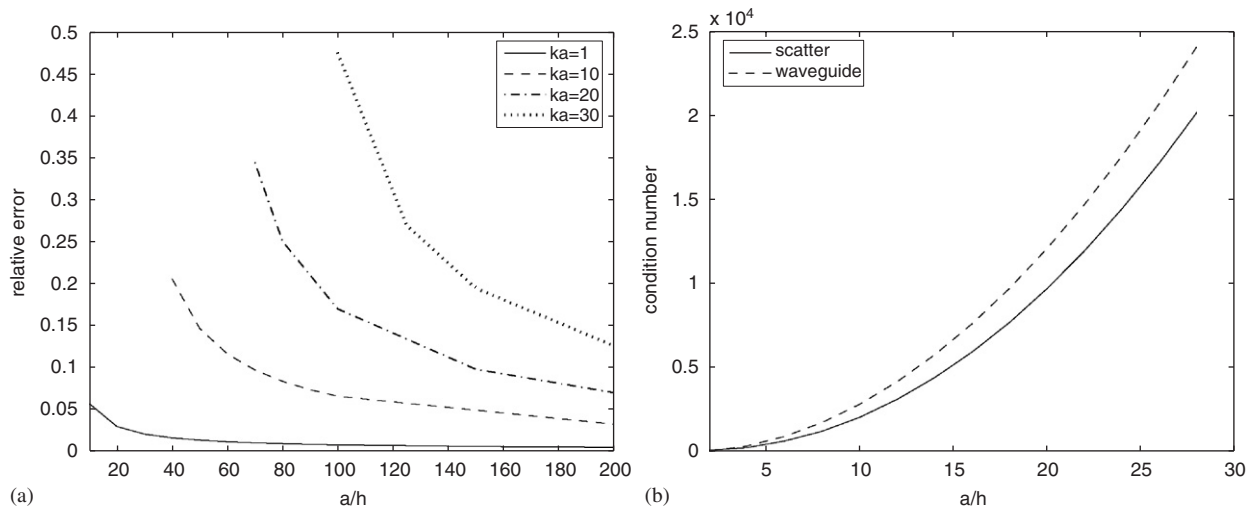


Fig. 2. Pollution effect.

Fig. 3. Sensitivity of the relative error to the frequency and the mesh size: (a) Dependence with respect to ka ; (b) Mesh resolution required for a fixed 10% total relative error.

- ii. When ka increases and h decreases, while maintaining kh constant ($kh = \frac{1}{5}$), the method exhibits little pollution (less than 1% for any propagation angle θ^*). More precisely, we observe that in the interval $[0, \pi)$ of the propagation angle, the maximum of the pollution is reached at $\theta^* = 0^\circ$ (the increase in the relative error is about 0.7%). The pollution is minimal at the propagation angle $\theta^* = 130^\circ$ (the increase in the relative error is about 0.3%).
- b. In Fig. 3(a), we report the results obtained for three different values of the mesh size $h/a = \frac{1}{25}, \frac{1}{50}, \frac{1}{100}$ as the value of ka increases. Fig. 3(a) illustrates the accuracy performance of the proposed method. Indeed, it shows that the total relative error is divided by almost a factor of 2 as h/a is divided by 2. This result tends to indicate that the total relative error depends quasi-linearly with kh .
- c. The result reported Fig. 3(b) shows that it is enough to maintain $kh = \frac{1}{5}$ to achieve a level of accuracy less than 10% when ka increases.

Fig. 4. Mesh partition of the computational domain for $N = 2$.Fig. 5. (a) Relative error for a *sound-hard* circular-shaped scatterer; (b) condition number comparison for $ka = 1$.

4.1.2. Scattering waves by a disk

We consider now the case of scattering waves by a *sound-hard circular-shaped* scatterer. We reformulate this classical exterior Helmholtz problem in a *bounded* domain as BVP (1) where the interior boundary Γ is a circle of radius a and the exterior boundary Σ is chosen to be a circle of radius r_1 ($0 < a < r_1$). In order to take into account the spurious numerical reflections of waves due to the boundary condition applied on Σ , we consider the Fourier series solution of BVP (1) (see Ref. [13] among others).

$$u^{\text{ex}}(r, \theta) = 2 \sum_{m=0}^{\infty} {}' (-i)^m (A_m^2 H_m^1(kr) + A_m^1 H_m^2(kr)) \cos(m\theta), \quad (10)$$

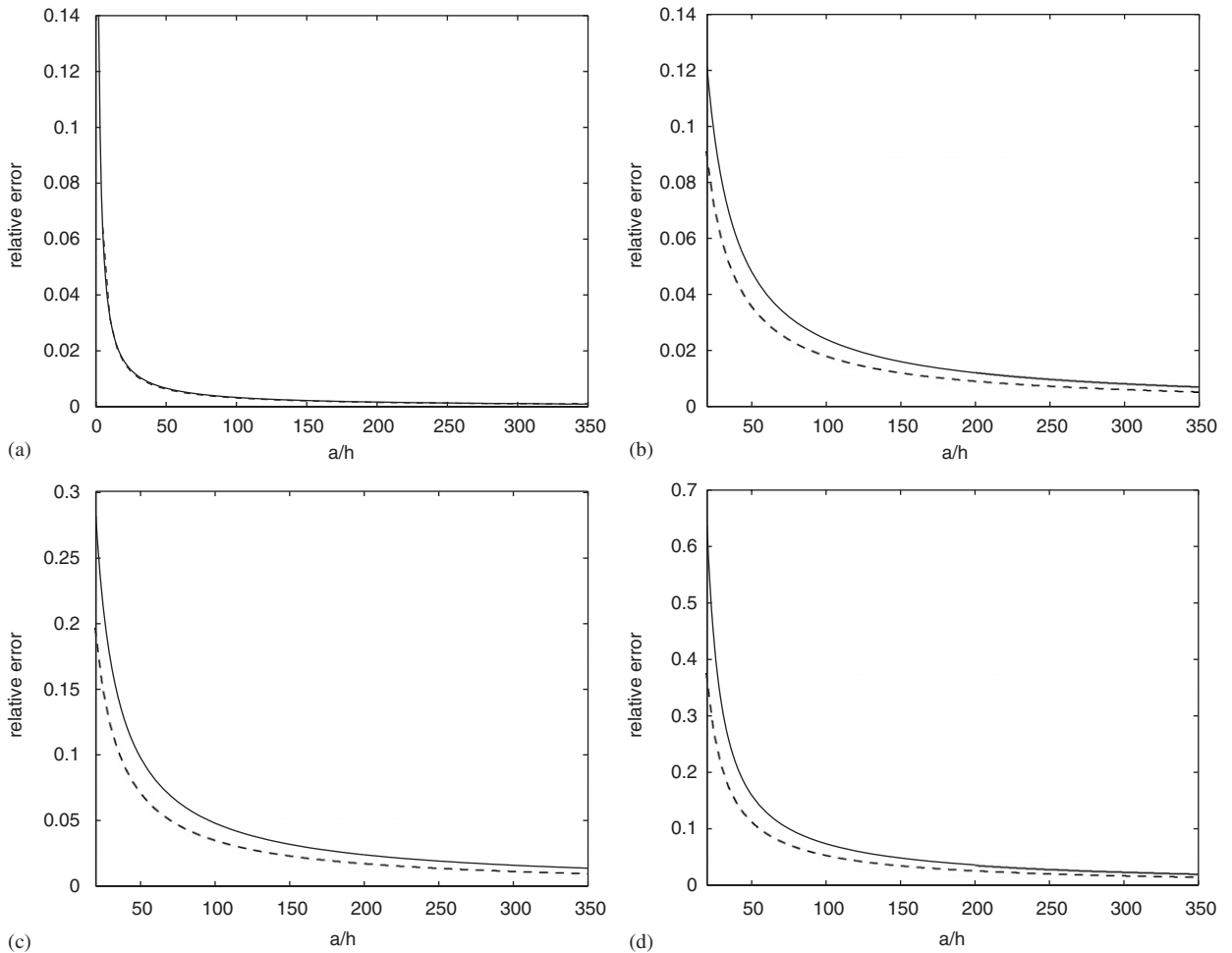
where the prime on the sum indicates that the first term is halved and the Fourier coefficients A_m^l are given by

$$A_m^l = (-1)^l \frac{J_m'(ka)}{\Delta_m} (H_m^{l'}(kr_1) - i H_m^l(kr_1)); \quad l = 1, 2$$

Table 1

Relative error for a fixed mesh size $a/h = 200$

ka	Relative error (%)
1	0.43
10	3.19
20	6.99
30	12.56

Fig. 6. Performance comparison: — oscillated polynomial, - - - planar element: (a) $ka = 1$; (b) $ka = 10$; (c) $ka = 20$; (d) $ka = 30$.

and

$$\Delta_m = H_m^{1'}(ka)(H_m^{2'}(kr_1) - iH_m^2(kr_1)) - H_m^{2'}(ka)(H_m^{1'}(kr_1) - iH_m^1(kr_1)).$$

Here J_m are m -order Bessel functions and H_m^1 (resp. H_m^2) are m -order Hankel functions of the first kind (resp. the second kind) [1].

We generate the partition of the computational domain Ω^c in triangular-shaped elements as follows (see Fig. 4). We first divide the radial interval direction $[a, r_1]$ is divided equally in N subintervals. Then, the angular direction $0 \leq \theta \leq 2\pi$ is divided equally in $4N$ domains. Last, we “halve” the resulting quadrilateral-shaped elements as illustrated in Fig. 4

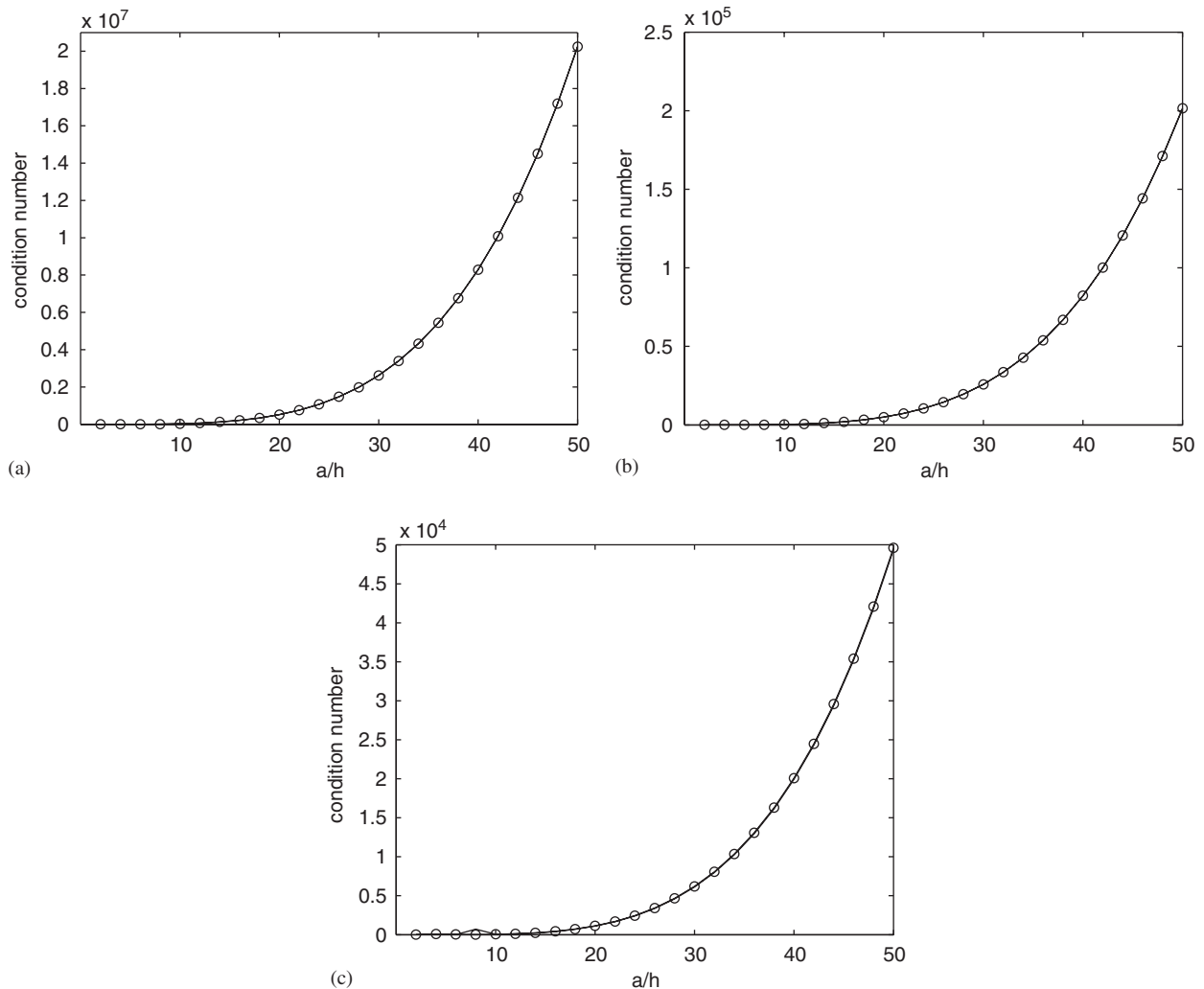


Fig. 7. Condition numbers: — oscillated polynomial, -o-o-o- planar element: (a) $ka = 1$; (b) $ka = 10$; (c) $ka = 20$.

to generate the triangular-shaped domains. The mesh step size h satisfies $h/a = 1/N$. We have performed numerical experiments to assess the accuracy of the method. The results reported in Fig. 5(a) are obtained for the following frequencies $ka = 1, 10, 20, 30$. We have computed the relative error in the modified H^1 norm (see Eq. (9)) by using up to 45 terms in the Fourier series (depending on the frequency ka) to compute the exact solution (see Eq. (10)). Note that in all the numerical experiments, the artificial boundary Σ was located at $r_1 = 2a$. The following observations are noteworthy:

- Fig. 5(a) reveals that for a fixed discretization mesh h , the relative error is *asymptotically* “almost” linear with respect to the frequency ka . This is clearly illustrated in Table 1 for $h/a = 200$ where we can observe that the relative error increases with the increase rate of the frequency.
- Fig. 5(a) also indicates that for a fixed discretization frequency ka , the relative error is *asymptotically* “almost” linear with respect to the mesh size h . For example, for $ka = 10$, the relative error corresponding to the mesh size $a/h = 100$ is 6.51%. This error is reduced by a factor 2 to 3.19% when the mesh is refined by a factor 2 ($a/h = 200$).
- We found (see Fig. 5(b)) that the condition number is comparable to the condition number in the case of the wave guide problem considered in the previous numerical experiment.

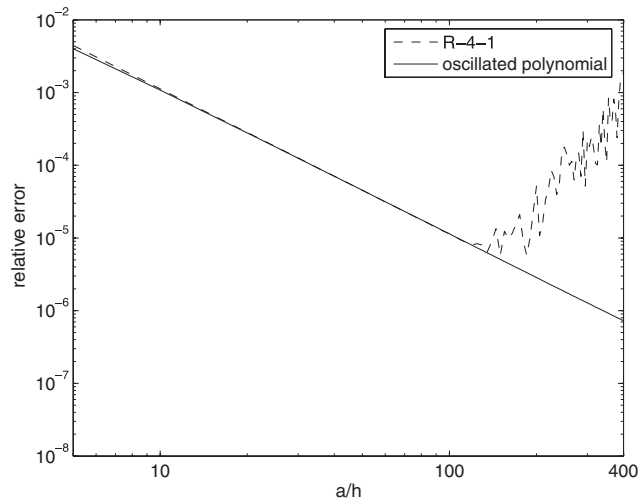


Fig. 8. Relative error in the L2 norm for $ka = 1$.

4.2. Comparison results

Next, we compare the performance of the proposed solution method with the DGM formulation proposed by Farhat et al. in [9] in the case of the so-called R-4-1 element. We must recall that the two solution methodologies are very similar. The only and main difference is in the approximation of the primal variable u at the element level. Indeed, DGM uses planar waves to approximate locally u (four orthogonal planar waves in the case of R-4-1 element). We perform the comparison when solving the waveguide problem described earlier (see Section 4.1). The computational domain here is also an $a \times a$ square-shaped domain, but we solve the Helmholtz equation with boundary conditions such that the exact solution u^{ex} of the resulting problem is of the form:

$$u^{\text{ex}} = e^{ikxy}. \quad (11)$$

We have chosen to use the exact solution given by Eq. (11) because the plane waves are used as shape functions in the DGM formulation. In addition, since DGM has been designed for quadrilateral-shaped elements only, we have used a uniform *rectangular*-shaped mesh to be able to compare the two methods. We recall in the case of the R-4-1 element, DGM performs 40 times better than standard Q_1 elements [9]. We report in Figs. 6 and 7 the preliminary results of this comparison analysis. The following three observations are noteworthy:

- Fig. 6 shows the sensitivity of the relative error with respect to mesh size of each method for a fixed wave number ka . The results indicate that both methods deliver a comparable level of accuracy.
- The condition number of the system resulting from the static condensation procedure in both methods produced is identical in the frequency regime $ka \in [1, 30]$ as indicated in Fig. 7.
- The comparison of both methods for finer meshes in the case of $ka = 1$ reveals that the DGM method exhibits a locking phenomenon, as illustrated in Fig. 8, while our method produces a perfectly “flat” curve. This locking, which has been already observed for higher elements (Q-32-8) in [11], seems to be related to the deterioration of the condition number of the element-level matrix in the condensation process.

5. Summary and conclusion

A new mixed-hybrid-type method based on (a) the local approximation of the solution by oscillated finite elements and (b) the use of Lagrange multipliers to “weakly” enforce continuity across element boundaries is proposed to solve Helmholtz problems in the mid- and high-frequency regime. This method is very similar to the DGM formulation which uses planar waves to approximate locally the solution. The proposed method combines the features of finite elements

techniques in terms of implementation and the oscillating aspect of the solution. In addition, unlike DGM method, the proposed method can be formulated using either triangular- or quadrilateral-shaped elements with no additional difficulties. Another interesting feature of the proposed method is that its extension to three-dimensional problems is conceptually—at least—straightforward. Additionally, unlike our solution methodology, the DGM formulation exhibits a locking phenomenon which may hamper its performance for very fine mesh that are needed in the high-frequency regime. There are still many remaining issues chief among them a numerical investigation in the case of acoustic scattering problems, the establishment of error estimates, and the use of higher-order elements for approximating the Lagrange multipliers as well as for approximating the solution. Nonetheless, the preliminary results presented in this paper illustrate the potential of this method for solving Helmholtz problems in the mid- and high-frequency regime.

Acknowledgments

The authors acknowledge partial support by the National Science Foundation under Grant No. DMS-0406617, and partial support by the Office of Graduate Studies at California State University Northridge (CSUN). Any opinions, findings, and conclusions or recommendations expressed in this material are those of the authors and do not necessarily reflect the views of the National Science Foundation, or CSUN.

References

- [1] M. Abramowitz, I.A. Stegun, *Handbook of Mathematical Functions*, US Department of Commerce, National Bureau of Standards, 1972.
- [2] M. Amara, R. Djellouli, C. Farhat, Convergence analysis of a discontinuous Galerkin method with plane waves and Lagrange multipliers for the solution of Helmholtz problems, *SIAM J. Numer. Anal.*, submitted for publication.
- [3] I. Babuška, F. Ihlenburg, E.T. Paik, S.A. Sauter, A generalized finite element method for solving the Helmholtz equation in two dimensions with minimal pollution, *Comput. Methods Appl. Mech. Eng.* 128 (1995) 325–359.
- [4] I. Babuška, I.J.M. Melenk, The partition of unity method, *Internat. J. Numer. Methods Eng.* 40 (1997) 727–758.
- [5] I. Babuška, S.A. Sauter, Is the pollution effect of the FEM avoidable for the Helmholtz equation considering high wave numbers, *SIAM J. Numer. Anal.* 34 (1997) 2392–2423.
- [6] F. Brezzi, M. Fortin, *Mixed and Hybrid Finite Element Methods*, Springer, Berlin, 1991.
- [7] O.P. Bruno, L.A. Kunyansky, High-order algorithm for the solution of surface scattering problems: basic implementation, tests, and applications, *J. Comput. Phys.* 169 (2001) 80–110.
- [8] O. Cessenat, B. Despres, Application of an ultra weak variational formulation of elliptic PDEs to the two-dimensional Helmholtz problem, *SIAM J. Numer. Anal.* 35 (1998) 255–299.
- [9] C. Farhat, I. Harari, U. Hetmaniuk, A discontinuous Galerkin method with Lagrange multipliers for the solution of Helmholtz problems in the mid-frequency regime, *Comput. Methods Appl. Mech. Eng.* 192 (2003) 1389–1419.
- [10] C. Farhat, R. Tezaur, P. Wiedemann-Goiran, Higher-order extensions of a discontinuous Galerkin method for mid-frequency Helmholtz problems, *Internat. J. Numer. Methods Eng.* 61 (2004) 1938–1956.
- [11] C. Farhat, P. Weidemann-Goiran, R. Tezaur, A discontinuous Galerkin method with plane waves and Lagrange multipliers for the solution of short wave exterior Helmholtz problems on unstructured meshes, *Wave Motion* 39 (2004) 307–317.
- [12] L.P. Franca, C. Farhat, A.P. Macedo, M. Lesoinne, Residual-free bubbles for the Helmholtz equation, *Internat. J. Numer. Methods Eng.* 40 (1997) 4003–4009.
- [13] A. Gillman, On the numerical performance of a mixed-hybrid type solution methodology for solving high-frequency Helmholtz problems, Master's Thesis, California State University Northridge, June 2006.
- [14] I. Harari, T.J.R. Hughes, Galerkin/least-squares finite element methods for the reduced wave equation with non-reflecting boundary conditions in unbounded domains, *Comput. Methods Appl. Mech. Eng.* 98 (1992) 411–454.
- [15] (<http://www.computational.unibas.ch/cs/scicomp/software/pardiso/6>).
- [16] T. Huttunen, P. Monk, J.P. Kaipio, Computational aspects of the ultra-weak variational formulation, *J. Comput. Phys.* 182 (2002) 27–46.
- [17] O. Laghrouche, P. Bettess, Short wave modelling using special finite elements, *J. Comput. Acoust.* 8 (2000) 189–210.
- [18] P. Monk, D.Q. Wang, A least-squares method for the Helmholtz equation, *Comput. Methods Appl. Mech. Eng.* 175 (1999) 121–136.
- [19] M.E. Rose, Weak element approximations to elliptic differential equations, *Numer. Math.* 24 (1975) 185–204.
- [20] R. Tezaur, A. Macedo, C. Farhat, R. Djellouli, Three-dimensional finite element calculations in acoustic scattering using arbitrarily shaped convex artificial boundaries, *Internat. J. Numer. Methods Eng.* 53 (2002) 1461–1476.